Molecular Crystals and Liquid Crystals
Publication details, including instructions for authors and subscription information:
http://www.tandfonline.com/loi/gmcl20

Influence of Terminal Groups on the Mesogenic Properties of Self-Assembly Systems

N. Pongali Sathya Prabu [a], V. N. Vijayakumar [a] & M. L. N. Madhu Mohan [a]

[a] Liquid Crystal Research Laboratory (LCRL), Bannari Amman Institute of Technology, Sathyamangalam, India

Version of record first published: 07 Oct 2011

To cite this article: N. Pongali Sathya Prabu, V. N. Vijayakumar & M. L. N. Madhu Mohan (2011): Influence of Terminal Groups on the Mesogenic Properties of Self-Assembly Systems, Molecular Crystals and Liquid Crystals, 548:1, 142-154

To link to this article: http://dx.doi.org/10.1080/15421406.2011.591682

Mol. Cryst. Liq. Cryst., Vol. 548: pp. 142–154, 2011

ISSN: 1542-1406 print/1563-5287 online
DOI: 10.1080/15421406.2011.591682

Influence of Terminal Groups on the Mesogenic Properties of Self-Assembly Systems

N. PONGALI SATHYA PRABU, V. N. VIJAYAKUMAR, AND M. L. N. MADHU MOHAN*

Liquid Crystal Research Laboratory (LCRL), Bannari Amman Institute of Technology, Sathyamangalam, India

Two novel hydrogen-bonded liquid crystal homologous series are synthesized and characterized. A hydrogen bond is formed between various p-n alkyloxy benzoic acids and chloro/hydroxy benzaldehyde. The formation of hydrogen bonds is evinced through Fourier Infra Red Spectroscopy studies. The terminal group of the aldehyde group has been varied and the thermal, optical, and electrical results are compared and analyzed. Both series exhibit rich liquid crystalline-phase polymorphism. Phase diagrams are constructed from the Differential Scanning Calorimetry and optical polarizing microscopic data. The phase sequence is same for both the series, with nematic, smectic C, and smectic G phases. A noteworthy point is the observation of optical shuttering action in the homologous series with the chloro terminal group of the aldehyde group and absence of the same in the other homologous series. The influence of terminal group of the aldehyde group with respect to occurrence of phase variance, tilt angle, optical shuttering action, and odd–even effect is discussed.

Keywords Hydrogen-bonded liquid crystal; odd–even effect; optical shuttering action; phase variance

1. Introduction

Liquid crystals are the intermediate state of matter between molecularly oriented solid and free flow liquids. They are mostly formed by the intermolecular hydrogen bonding between the complexes which prompted scientists to turn their interest toward hydrogen bonding. Kato and his coworkers [1–8] investigated many such systems with complementary components. It is noteworthy that it is not necessary that both of the complexes exhibit mesogenic properties. To induce mesomorphic state, various molecular interactions, such as charge transfer and ionic–dipolar interactions between the different molecular species, have been used. Normally, to obtain the enormous use of hydrogen-bonded liquid crystals, the mesogens containing only two aromatic rings have been used to stimulate room temperature mesogens. Hydrogen bonding is one of the prime interactions for chemical and biological processes in nature due to its directionality and dynamics. Hydrogen bonding plays a vital role in the association of molecules for molecular aggregation.

*Address correspondence to M. L. N. Madhu Mohan, Liquid Crystal Research Laboratory (LCRL), Bannari Amman Institute of Technology, Sathyamangalam 638 401, India. Tel.: +91-4295-223-480; Fax: +91-4295-223-775. E-mail: mln.madhu@gmail.com

The chemical molecular design of liquid crystal mesogen plays a vital role in understanding the various mesogenic and other physical properties exhibited by it. From the literature, it can be inferred that various moieties of the chemical structure contribute to various properties exhibited by the mesogen. The transverse and longitudinal dipoles have greater impact on the conjugation and the electrical properties. Thus, the engineering of the molecular structure for the desired properties is an interesting aspect from the applicational point of view.

We have already reported [9–17] single, double, and multiple hydrogen bond formation between the mesogenic and nonmesogenic complexes. The self-assembly systems formed by alkyloxy carboxylic acids exhibit rich phase polymorphism. It has previously been reported by us that these self-organized systems induce variety of new phenomena like reentrant phase occurrence [9,10], light modulation [11], optical shuttering action [12–15], and field-induced transitions [11,16,17]. A successful attempt has been made to understand the influence of the terminal groups (OH and Cl) on the self-assembly system comprising of aldehyde and alkyloxy benzoic acids.

2. Experimental

Optical textural observations are made with a Nikon polarizing microscope equipped with Nikon (Japan) digital CCD camera system with 5 megapixels and 2560 × 1920 pixel resolutions. The temperature control is equipped with Instec HCS402-STC 200 (USA) temperature controller to a resolution of $\pm 0.1^{\circ}$C. The liquid crystal sample is filled by capillary action in its isotropic state into a commercially available (Instec, USA) polyamide buffed cell with 5 micron spacer. An optical extinction technique [18] is used for the determination of tilt angle. Transition temperatures and corresponding enthalpy values are obtained by Differential Scanning Calorimetry (DSC) (Shimadzu DSC-60, Japan) while Fourier Infra Red Spectroscopy (FTIR) spectra is recorded (ABB FTIR MB3000, Canada) and analyzed using the MB3000 software. The *p*-*n*-alkyloxy benzoic acids (*n*BA) and hydroxy and chloro benzaldehyde are supplied by Sigma Aldrich (Germany) and all the solvents used are HPLC grade.

2.1 Synthesis of Liquid Crystalline Compounds

Intermolecular hydrogen-bonded mesogens are synthesized by the addition of one mole of *p*-*n*-alkyloxy benzoic acids with one mole of chlorobenzaldehyde/hydroxybenzaldehyde in *N*, *N*-dimethyl formamide (DMF). Further, they are subject to constant stirring for 12 h at ambient temperature (30°C) till a white precipitate in a dense solution is formed. The white crystalline crude complexes are obtained by removing excess DMF recrystallized with dimethyl sulfoxide (DMSO) and the yield varied from 75% to 99%. The molecular structures of the present homologous series of *p*-*n*-alkyloxy benzoic acids with chlorobenzaldehyde (CBA+nBAO)/hydroxybenzaldehyde (HBA+nBAO) are depicted in Figs. 1(a) and (b), respectively, where *n* represents the alkyloxy carbon number. Thus, the above two series of hydrogen-bonded complexes are labeled as CBA+nBAO and HBA+nBAO, respectively.

3. Results and Discussion

The synthesized hydrogen-bonded liquid crystals are highly stable at ambient temperature (30°C). They show high thermal and chemical stability when subjected to repeated thermal scans performed during polarizing optical microscopic (POM) and DSC studies.

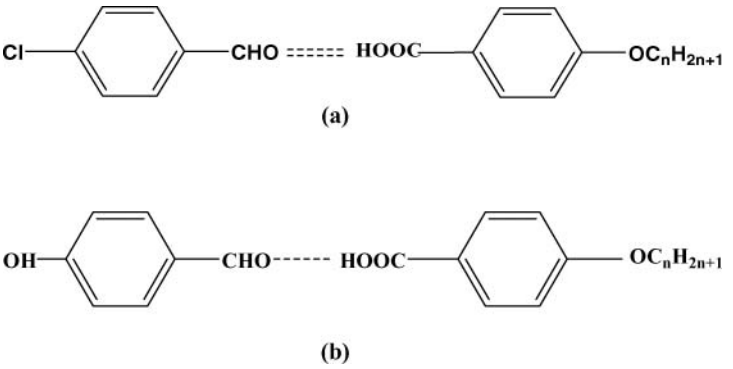

Figure 1. Molecular structure of (a) CBA+nBAO series and (b) HBA+nBAO series.

3.1 Phase Identification

The observed phase variants, transition temperatures, and corresponding enthalpy values of CBA+nBAO and HBA+nBAO obtained by DSC in cooling and heating cycles for the complexes are presented in Tables 1(a) and (b), respectively.

3.2 Polarizing Optical Microscopic Studies (POM)

The above hydrogen-bonded complexes are found to exhibit characteristic textures [19], viz., nematic (threaded texture), smectic C (broken focal conic texture), and smectic G (mosaic texture), respectively. The general phase sequence of the present hydrogen-bonded complexes in the cooling run is observed as:

Isotropic → Nematic → SmC → SmG → Crystal CBA + nBAO (n = 7 − 12)
Isotropic → Nematic → SmG → Crystal CBA + 6BAO
Isotropic → Nematic → Crystal CBA + 5BAO
Isotropic → Nematic → SmG → Crystal HBA + nBAO (n = 5, 6)
Isotropic → Nematic → SmC → SmG → Crystal HBA + nBAO (n = 7 − 12).

3.3 Infrared Spectroscopy (FTIR)

Figure 2 illustrates the solid state spectra, i.e., FTIR spectra of the hydrogen-bonded CBA+12BAO complex in solid state, at room temperature (30°C) as a representative case. The solid state spectra of *p-n* alkyloxy benzoic acid is reported [11,20] to have two sharp bands at 1685 cm^{-1} and 1695 cm^{-1} due to the frequency ν(C=O) mode. The doubling feature of this stretching mode confirms the dimeric nature of alkyloxy benzoic acid at room temperature [20]. Further, in the present CBA+12BAO hydrogen-bonded complex, a band appearing at 2924 cm^{-1} is assigned to ν(O-H) mode of the carboxylic acid group while bands appearing at 1605 cm^{-1} and 1680 cm^{-1} are assigned to ν(C=O) mode. Various bands of ν(O-H) and ν(C=O) modes corresponding to individual complexes of CBA+nBAO and HBA+nBAO are tabulated in Table 2.

Table 1. Transition temperatures and enthalpy values of CBA+nBAO series obtained by various techniques

Complex	Phase variance	Study	Crystal to melt	N	C	G	Crystal
CBA +5BAO	N	DSC (H)	114.2 (116.55)	143.4 (9.28)			
		DSC (C)		145.8 (8.71)			107.0 (105.24)
		POM (C)		146.3			107.8
CBA +6BAO	NG	DSC (H)	94.9 (40.11)	151.2 (4.61)			
		DSC (C)		146.7 (9.00)		87.3 (Merged with crystal)	85.4 (36.35)
		POM (C)		147.2		87.9	86.6
CBA +7BAO	NG	DSC (H)	89.8 (142.22)	144.6 (7.16)		#	
		DSC (C)		141.5 (5.95)		81.5 (1.62)	71.1 (105.7)
		POM (C)		142.4		82.1	71.8
CBA +8BAO	NCG	DSC (H)	77.4 (54.49)	146.95 (7.9)	98.3 (2.39)	90.9 (17.98)	
		DSC (C)		143.3 (7.35)	97.9 (2.81)	87.9 (20.49)	56.7 (38.43)
		POM (C)		144.7	98.5	88.3	57.6
CBA +9BAO	NCG	DSC (H)	93.4 (121.8)	140.6 (8.98)	114.7 (3.4)	#	
		DSC (C)		136.1 (8.56)	109.4 (3.55)	81.8 (16.04)	67.8 (70.36)
		POM (C)		136.8	110.3	82.2	68.6
CBA +10BAO	NCG	DSC (H)	87.3 (143.08)	140.6 (13.18)	116.09 (3.49)	#	
		DSC (C)		137.5 (9.6)	112.4 (3.22)	82.8 (26.3)	67.1 (28.47)
		POM (C)		138.2	113.1	83.4	67.9
CBA +11BAO	NCG	DSC (H)	96.9 (135.84)	139.9 (6.83)	127.3 (5.47)	#	
		DSC (C)		136.9 (7.85)	124.2 (3.47)	80.0 (25.23)	70.3 (27.39)
		POM (C)		137.7	124.9	80.8	71.1
CBA +12BAO	NCG	DSC (H)	94.53 (127.25)	137.1 (3.43)	#	100.2 (5.15)	
		DSC (C)		132.3 (6.69)	126.3 (2.88)	80.1 (23.22)	68.6 (81.6)
		POM (C)		132.9	127.5	80.9	69.7

Phase not resolved; (H) heating run, (C) cooling run.

Table 2. Transition temperatures and enthalpy values of HBA+nBAO series obtained by various techniques

Complex	Phase variance	Study	Crystal to melt	N	C	G	Crystal
HBA+12BAO	NCG	DSC (h)	107.7 (44.30)	#	#	#	
		DSC (c)		109.4 (7.77)	87.3 (merged with G)	84.2 (19.76)	81.1 (39.60)
		POM (c)		110.8	88.1	84.9	81.8
HBA +11BAO	NCG	DSC (h)	107.0 (23.09)	#	#	#	
		DSC (c)		118.6 (0.06)	114.2 (0.23)	108.0 (4.85)	91.4 (112.69)
		POM (c)		119.5	115.1	108.7	91.8
HBA +10BAO	NCG	DSC (h)	85.6 (41.17)	114.5 (1.26)	#	95.8 (20.78)	
		DSC (c)		111.1 (0.13)	108.2 (6.14)	92.6 (merged with crystal)	82.5 (22.41)
		POM (c)		112.9	109.3	93.5	82.9
HBA +9BAO	NCG	DSC (h)	93.6 (62.85)	#	#	#	
		DSC (c)		106.5 (3.83)	90.3 (17.35)	74.3 (33.14)	62.0 (43.27)
		POM (c)		107.8	91.7	74.9	62.4
HBA +8BAO	NCG	DSC (h)	100.0 (36.23)	#	#	#	
		DSC (c)		116.3 (merged with C)	101.4 (1.44)	94.8 (25.64)	75.1 (27.96)
		POM (c)		117.6	102.9	95.3	75.5
HBA +7BAO	NCG	DSC (h)	92.4 (79.88)	#	#	#	
		DSC (c)		106.1 (0.03)	99.7 (0.97)	88.2 (24.27)	83.3 (93.05)
		POM (c)		107.5	100.9	89.1	83.8
HBA +6BAO	NG	DSC (h)	101.2 (36.56)	#		#	
		DSC (c)		107.7 (1.04)		93.2 (30.47)	83.5 (38.60)
		POM (c)		108.8		94.3	84.0
HBA +5BAO	NG	DSC (h)	104.3 (73.07)	#		114.7 (21.31)	
		DSC (c)		122.1 (merged with G)		110.2 (50.61)	88.0 (56.77)
		POM (c)		123.2		111.4	88.7

Phase not resolved; (H) heating run, (C) cooling run.

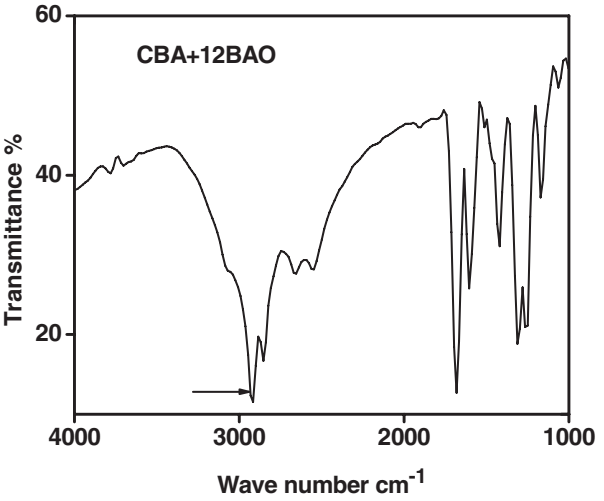

Figure 2. FTIR spectra of the CBA+12BAO complex.

3.4 DSC Studies

DSC thermograms for all the complexes have been recorded at a scan rate of 10°C min^{-1} for the heating and cooling runs, and analyzed. The transition temperatures and enthalpy values for all the homologues of CBA+nBAO and HBA+nBAO are tabulated in Tables 1(a) and (b), respectively.

As a representative case, Fig. 3 illustrates the thermogram of CBA+9BAO hydrogen-bonded complex recorded at a scan rate of 10°C min^{-1} in the heating and cooling runs. In the cooling run of DSC thermogram, the above compound possesses four distinct transitions namely isotropic to nematic, nematic to Sm C, Sm C to Sm G, and Sm G to crystal with transition temperatures 136.1°C, 109.4°C, 81.8°C, and 67.8°C, and corresponding enthalpy values 8.56 J g^{-1}, 3.55 J g^{-1}, 16.04 J g^{-1}, and 70.36 J g^{-1}, respectively. While in the heating cycle, three distant transitions namely crystal to melt, melt to Sm G, and Sm G to Sm C

Table 2. FTIR data representing the various modes for CBA+nBAO and HBA+nBAO homologous series, respectively

	υ(OH)	υ (CO)		υ(OH)	υ (CO)	
Compound	CBA+nBAO			HBA+nBAO		
5BAO	2933	1605	1690	2955	1597	1682
6BAO	2933	1605	1690	2939	1597	1682
7BAO	2932	1605	1674	2932	1605	1674
8BAO	2927	1605	1692	2932	1605	1674
9BAO	2924	1605	1682	2924	1605	1674
10BAO	2924	1605	1680	2924	1605	1674
11BAO	2924	1608	1680	2924	1605	1674
12BAO	2924	1605	1680	2924	1605	1674

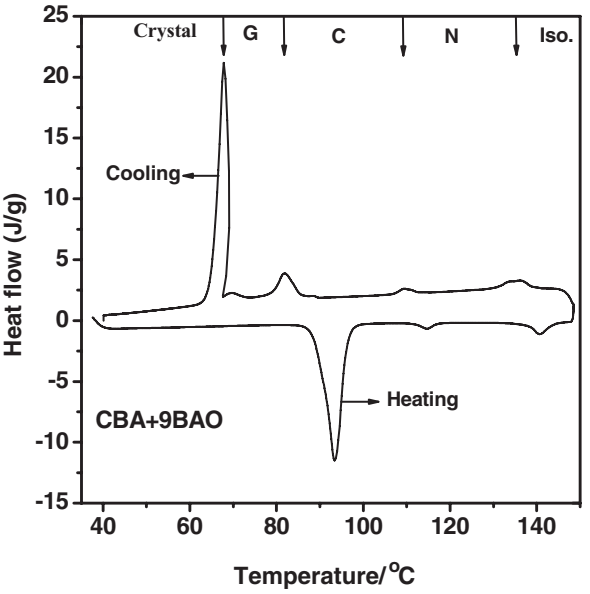

Figure 3. DSC thermogram of the CBA+9BAO complex.

are obtained at 93.4°C, 140.6°C, and 114.7°C with corresponding enthalpy values of 121.8 J g^{-1}, 8.98 J g^{-1}J/g, and 3.4 J/g, respectively.

The transition temperatures and enthalpy values for other hydrogen-bonded complexes are analyzed and represented in Table 1. All of these transition temperatures of the present homologous series concur with POM studies.

3.5 Phase Diagrams

3.5.1 Pure p-n-Alkyloxy Benzoic Acids. The phase diagram of pure *p-n*-alkyloxy benzoic acid is reported [9,14] to be composed of two phases, namely nematic and smectic C.

3.5.2 CBA+nBAO Series. The phase diagram of CBA+nBAO series is depicted in Fig. 4 which reveals the following points:

a) The phase diagram is composed of orthogonal and tilted phases, viz., nematic and Sm. C and Sm. G.
b) Nematic phase is observed in all the members of the present homologous series.
c) Odd–even effect is observed in transition temperatures of isotropic to nematic transition.
d) A noteworthy point is that at even carbon numbers, tilted phases are induced, viz., at the hexyloxy carbon number, Sm. G is induced while at octyloxy carbon number, smectic C phase is induced.
e) The thermal span of the nematic is found to be greatly reduced with the induction of the higher order smectic C phase.
f) The lower homologous have the larger thermal span of the nematic phase compared to their higher counterparts.

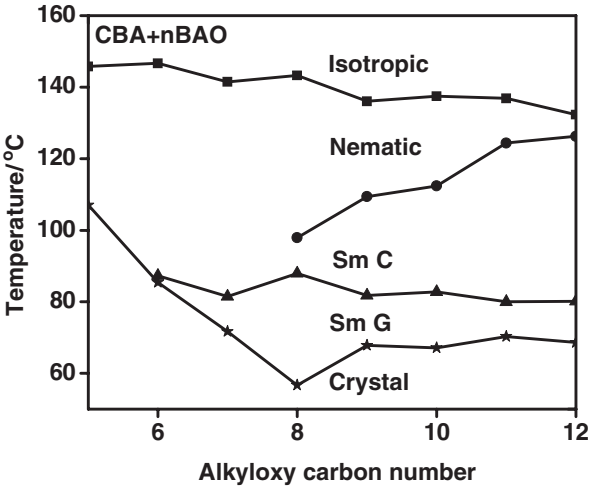

Figure 4. Phase diagram of the CBA+nBAO series.

g) The total mesogenic range in the present homologous series started to increase up to octyloxy carbon number and then it saturated with the further increment of the carbon number.

3.5.3 HBA+nBAO Series. The phase diagram of HBA+nBAO series is depicted in Fig. 5, which reveals the following points:

a) The HBA+nBAO hydrogen-bonded complex exhibits nematic as orthogonal phase and smectic C and smectic G as tilted phases.
b) The thermal range of the mesogenic phases increased with increase in the alkyloxy carbon number up to nonyloxy carbon and then starts to decrease till dodecyloxy benzoic acid.

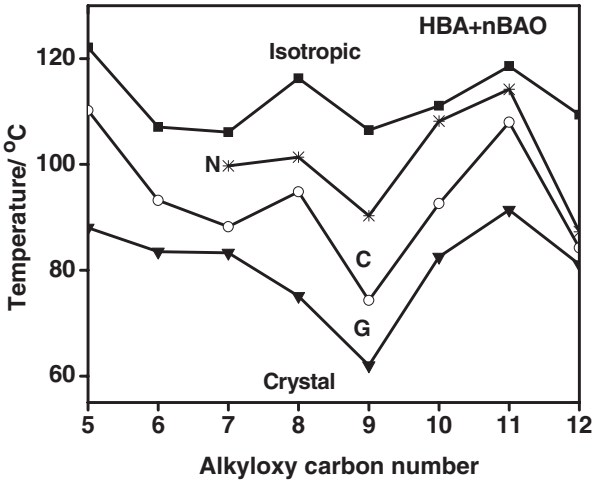

Figure 5. Phase diagram of the HBA+nBAO series.

c) Smectic G phase is observed in all the complexes of the present homologous series while ordered smectic C phase is induced in the higher homologous alkyloxy carbon numbers.
d) The liquid crystalline thermal range is largest for nonyloxy carbon and starts to reduce up to undecyloxy carbon.
e) A systematic decrease in the crystallization temperatures is observed up to nonyloxy benzoic carbon number. From then on, the crystallization temperatures start to increase proportionally along with its corresponding carbon number, with an exception of the dodecyloxy carbon number.

4. Odd–Even Effect in the Present Homologous Series

In the present homologous series, odd–even effect is noticed. Figure 6 depicts the variation of isotropic to nematic transition temperatures in HBA+nBAO and CBA+nBAO series. In the literature, such behavior has been reported [21] and is referred to as the odd–even effect. It may be noted that the present complex of liquid crystalline molecules is composed of rigid and flexible parts. The rigid core length varies with increment in the benzoic acid carbon number. The rich liquid crystalline phase polymorphism and the associated enthalpy values with increment of alkyloxy carbon number are thus attributed to this part of the chemical structure. Hence, the rigid core plays a vital role in establishing the pronounced odd–even effect as evinced in the present homologous series. A perfect zig-zag pattern is observed for the series with the choloro terminal group attached to the aldehyde group while for the other series, the odd–even effect is not so pronounced.

4.1 Optical Tilt Angle Studies in Smectic C

Optical tilt angle has been experimentally measured (Fig. 7) by the optical extinction method [18] in the smectic C phase of CBA+nBAO, ($n = 9$–12) and HBA+nBAO, ($n =$ 7–11) series, as shown in Figs. 7 and 8, respectively. From Figs 7 and 8, it is generally observed that the magnitude of the tilt angle increases with decreasing temperature and

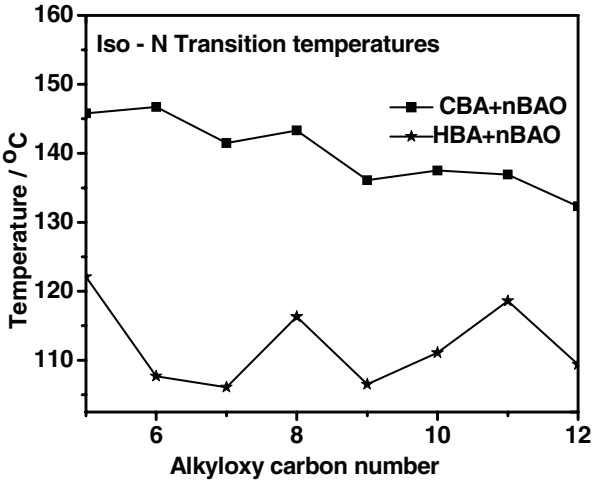

Figure 6. Odd – even effect at Iso-N transition temperature of CBA+nBAO and HBA+nBAO series.

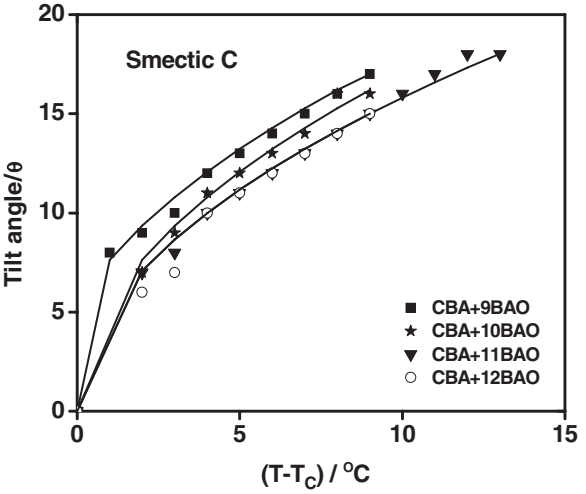

Figure 7. Tilt angle in smectic phase of CBA+nBAO series ($n = 9$–12).

attains a saturation value. The large magnitudes of the tilt angle are attributed [22] to the direction of the soft covalent hydrogen bond interaction which spreads along the molecular long axis with finite inclination. Tilt angle is a primary order parameter [21,23] and the temperature variation is estimated by fitting the observed data of θ (T) to the relation

$$\theta\ (T)\ \alpha\ (T - T_C)^{\beta}. \tag{1}$$

The critical exponent β value estimated by fitting the data of θ (T) to the above equation (1) is found to be 0.50 which agrees with the mean field theory [23] prediction. The solid lines in Figs 7 and 8 depict the fitted data. Furthermore, the agreement of β with

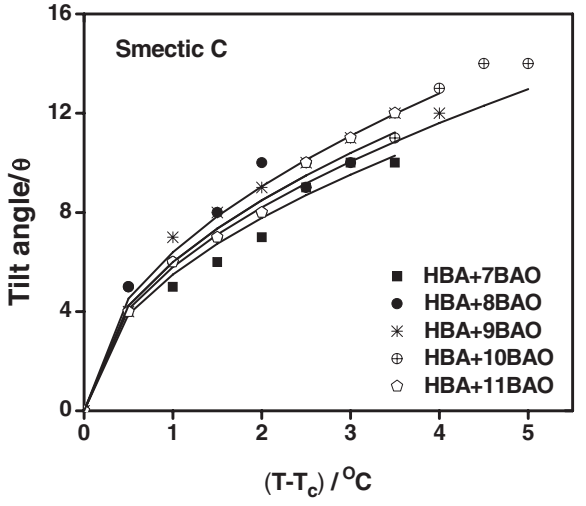

Figure 8. Tilt angle in smectic phase of HBA+nBAO series ($n = 7$–11).

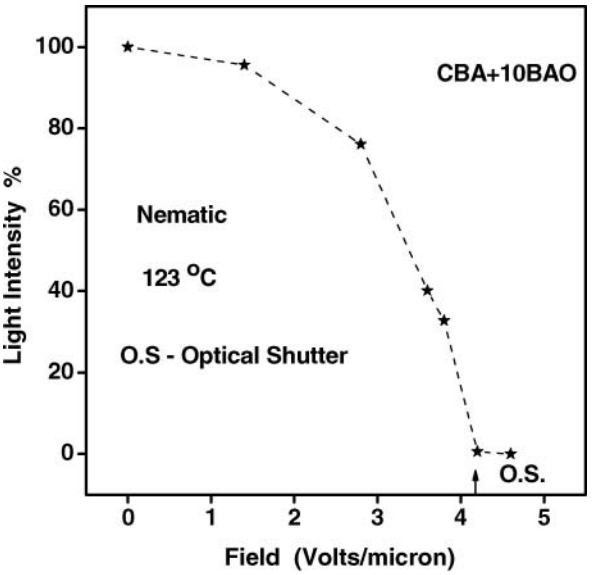

Figure 9. Light intensity versus applied field demonstration of optical shuttering in nematic of CBA+10BAO complex.

mean field theory value infers the long-range interaction of transverse dipole moment for the stabilization of tilted smectic phase.

4.2 Optical Shutter Action in CBA+10BAO

It is reported [24–33] that when a mesogen is subjected to an applied external field in cholesteric, nematic, or smectic C^* phase, there can be a phase transition. When the CBA+10BAO compound is in its nematic phase, i.e., when an applied dc bias voltage exceeds a particular threshold value, the phase of the compound is observed to prefer homeotropic-like alignment with light being optically extinct which is referred to as optical shutter. Figures 10(a)–(d) depict two regions of the nematic texture, one under the influence of various applied fields and the other with the nonconducting surface. It is interesting to note that immediately after withdrawing the bias voltage from the induced transition, the original texture of the nematic phase is retained. Thus, this process is reversible with bias voltage. In the entire thermal span of nematic phase, a $\sim$137°C to $\sim$112°C transition is observed. While in the other phases, i.e., the preceding and succeeding nematic phases, no such transition is found. Thus, the field-induced transitions can be represented as:

$$\mathbf{E_0} \rightarrow \textbf{Optical shutter } (\mathbf{E_1}).$$

A quantitative approach has been made to study the effect of applied electric field on hydrogen-bonded **CBA+10BAO** with optical textural and light intensity studies (Fig. 9). The nematic phase with a bias voltage (both polarities) less than or equal to $\pm$4.20 V micron^{-1} is referred to as $E_{0,}$ where there is no change in the texture of the smectic phase, as depicted in Fig. 10(a). As the voltage is increased in small steps, the intensity of the light from the texture drops, as can be seen from Figs. 10(b)–(d).

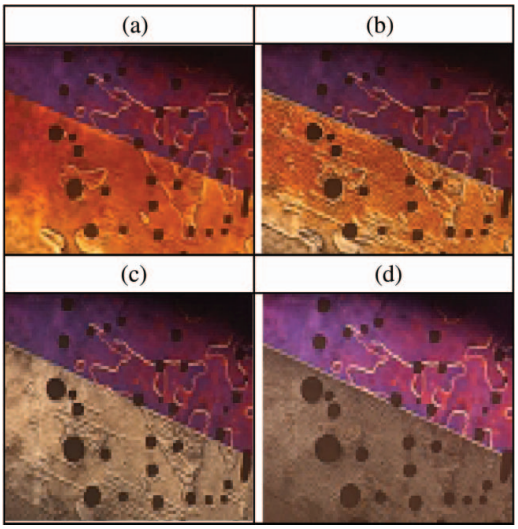

Figure 10. Nematic texture in conducting and nonconducting regions of CBA+10BAO (a) at a field of 0 V μ^{-1}, (b) at a field of 2.5 V μ^{-1}, (c) at a field of 4 V μ^{-1}, (d) at a field of 4.5 V μ^{-1}.

An important observation is that when a dc-bias voltage of ± 4.60 V micron^{-1} is applied, optical extinction is observed with the optical texture of the compound suddenly disappearing; this new phase is designated as optical shutter (E_1) which is depicted as Fig. 10(d). One of the possible reasons for this interesting phenomenon may be the realignment of the molecules to form a homeotropic-like alignment.

5. Effect of Terminal Groups

The following conclusions are drawn from the above results:

a) Terminal group chlorine favored phase variants of nematic, smectic C, and smectic G while the OH favored nematic, smectic C, and smectic F.
b) In both the series, higher order phases are induced in the higher homologues only.
c) Both the series exhibit odd–even effect in the isotropic to nematic transition temperature. However, it is more pronounced in the CBA+nBAO series.
d) By increasing alkyloxy carbon number, the mesogenic thermal range is increased in the CBA+nBAO, but the trend is reversed in the HBA+nBAO series.
e) The isotropic temperatures are more in the CBA+nBAO series when compared to HBA+nBAO series.
f) The CBA+nBAO series homologues exhibit larger magnitude of the tilt angle ($\sim 20^\circ$) compared to the HBA+nBAO series ($\sim 16^\circ$). The steric hindrances, which govern the molecular rotation, are more in the HBA+nBAO series.
g) The terminal group chlorine to the aldehyde favored optical shuttering action. This may be due to the high magnitude of electron negativity of the chlorine atom.

Acknowledgments

The authors acknowledge the financial support rendered by the Department of Science and Technology, Govt. of India. Infrastructural support provided by Bannari Amman Institute of Technology is gratefully acknowledged.

References

[1] Kato, T., & Frechet, J. M. J. (1995). *Macromol. Symp.*, *98*, 311.
[2] Kato, T., & Frechet, J. M. J. (1989). *J. Am. Chem. Soc.*, *111*, 8533.
[3] Kato, T., & Frechet, J. M. J. (1989). *Macromolecules*, *22*, 3818.
[4] Kato, T., Nakano, M., Moteki, T., Uryu, T., & Ujiie, S. (1995). *Macromolecules*, *28*, 8875.
[5] Kato, T., Frechet, J. M. J., Wilson, P. G., Saito, T., Uryu, T., Fujishima, A., Jin, C., & Kaneuchi, F. (1993). *Chem. Mater.*, *5*, 1094.
[6] Kato, T., Wilson, P. G., Fujishima, A., & Frechet, J. M. J. (1990). *Chem. Lett.*, *19*(11), 2003.
[7] Kato, T., Fukumasa, M., & Frechet, J. M. J. (1995). *Chem. Mater.*, *19*(11), *7*, 368.
[8] Fukumasa, T., Kato, T., Uryu, T., & Frechet, J. M. J. (1993). *Chem. Lett.*, *22*(1), 65.
[9] Vijayakumar, V. N., Mugugadass, K., & Madhu Mohan, M. L. N. (2010). *Mol. Cryst. Liq. Cryst.*, *43*, 517.
[10] Chitravel, T., & Madhu Mohan, M. L. N. (2010). *Mol. Cryst. Liq. Cryst.*, *524*, 131.
[11] Vijayakumar, V. N., & Madhu Mohan, M. L. N. (2009). *Ferroelectrics*., *392*, 81.
[12] Vijayakumar,V. N., & Madhu Mohan, M. L. N. (2010). *Mol. Cryst. Liq. Cryst.*, *517*, 113; (2010). *Mol. Cryst. Liq. Cryst.*, *524*, 54.
[13] Vijayakumar, V. N., & Madhu Mohan, M. L. N. (2009). *J. Optoelectron. Adv. Mater.*, *11*, 1139.
[14] Vijayakumar, V. N., & Madhu Mohan, M. L. N. (2009). *Braz. J. Phys.*, *39*, 677.
[15] Vijayakumar, V. N., & Madhu Mohan, M. L. N. (2010). *Mol. Cryst. Liq. Cryst.*, *528*, 163.
[16] Vijayakumar, V. N., & Madhu Mohan, M. L. N. (2009). *Solid State Sci.*, *12*, 482.
[17] Vijayakumar, V. N., & Madhu Mohan, M. L. N. (2009). *Solid State Commun.*, *149*, 2090.
[18] Noot, C., Perkins, S. P., & Coles, H. J. (2000). *Ferroelectrics*, *244*, 331.
[19] Gray, G. W., & Goodby, J. W. G. (1984). *Smetic Liquid Crystals – Textures and Structures*, Leonard Hill: London.
[20] Swathi, P., Sreehari Sastry, S., Kumar, P. A., & Pisipati, V. G. K. M. (2001). *Mol. Cryst. Liq. Cryst.*, *365*, 523.
[21] Chandrasekhar, S. (1977). *Liquid Crystals*, Cambridge University Press: New York.
[22] Barmatov, E. B., Bobrovsky, A., Barmatova, M. V., & Shibaev, V. P. (1999). *Liq. Cryst.*, *26*, 581.
[23] Stanley, H. E. (1971). *Introduction to Phase Transition and Critical Phenomena*, Clarendon Press: New York.
[24] Madhu Mohan, M. L. N., Kumar, P. A., & Pisipati, V. G. K. M. (1999). *Ferroelectrics*, *227*, 105.
[25] Kobayashi, S., & Ishibashi, S. (1994). *Mol. Cryst. Liq. Cryst.*, *257*, 181.
[26] Jong-Guang, W., & Shu-Hsia, C. (1994). *Jpn. J. Appl. Phys.*, *33*, 6249.
[27] Qian, T., & Taylor, P. L. (1999). *Phys. Rev. E*, *60*, 2978.
[28] Napoli, G. (2006). *J. Appl. Math.*, *71*, 34.
[29] Schlangen, L. J. M., Alexandre, P., & Cornelissen, H. J. (2000). *J. Appl. Phys.*, *87*, 3723.
[30] Hurd, A. J., Fraden, S., Lonberg, F., & Meyer, R. B. (1985). *J. Physique.*, *46*, 905.
[31] Zhang, S., Wen, B., Keast, S. S., Neubert, M. E., Taylor, P. L., & Rosenblatt, C. (2000). *Phys. Rev. Lett.*, *84*, 4140.
[32] Rotinyan, T. A., Ryumtsev, E. I., & Yazikov, S. B. (1987). *JETP Lett.*, *46*, 417.
[33] Cladiss, P. E., Garel, T., & Pieranski, P. (1986). *Phys. Rev. Lett.*, *57*, 2841.